A THERMO-HYDRO-MECHANICAL APPROACH FOR CRACKING AND ANISOTROPIC SHRINKAGE IN CELLULOSE-BASED POROUS MATERIALS

NAIMA BENMAKHLOUF,[*,**] ELTAYEB I. A. ELBESHIR[**,***] and MANEHIL HASSAN[**]

[*]*Laboratory of Energy and Thermal and Mass Transfers, Physics Department, Faculty of Science of Tunis, University of Tunis ElManar, 2092 El-Manar 2, Tunis, Tunisia*
[**]*Physics Department, Faculty of Science, Al-Baha University, Al-Baha P.O. Box 1988, Kingdom of Saudi Arabia*
[***]*Department of Physics and Applied Physics, Faculty of Science and Technology, Alneelain University, Khartoum, Sudan*
✉ *Corresponding author: N. Benmakhlouf, naima.benmakhlouf @fst.utm.tn*

Received October 3, 2025

Moisture removal in cellulose-based porous materials induces complex deformation phenomena driven by coupled heat transfer, moisture transport, and mechanical response. In this study, a fully coupled thermo-hydro-mechanical (THM) model is developed to investigate anisotropic shrinkage, stress evolution, and crack initiation during drying. The proposed framework integrates moisture-dependent transport properties, orthotropic elasticity, and a stress-based damage criterion within a unified finite element formulation.
The results show that moisture gradients are the dominant factor governing internal stress development, leading to significant tensile stress localization near exposed surfaces. The model successfully predicts anisotropic shrinkage behavior, with tangential (~9.2%) and radial (~4.3%) strains markedly exceeding longitudinal deformation (~0.2%). Damage analysis reveals that crack initiation occurs at intermediate drying stages and propagates inward following the moisture gradient. A parametric study demonstrates that moisture diffusivity and sample thickness are the most influential parameters controlling stress magnitude and failure risk, whereas thermal effects play a secondary role. Validation against literature data confirms the capability of the model to reproduce realistic drying-induced behavior in cellulose-based materials. The findings provide new insights into the coupled mechanisms governing deformation and damage, highlighting that failure is primarily transport-controlled. The proposed THM framework serves as a predictive and optimization tool for minimizing defects and improving the structural integrity of cellulose-based materials in industrial applications.

Keywords: cellulose, drying-induced cracking, anisotropic shrinkage, thermo-hydro-mechanical modeling, viscoelasticity, finite element analysis

INTRODUCTION

Cellulose-based porous materials, derived from the most abundant biopolymer on Earth, are widely used in a broad range of industrial applications, including paper manufacturing, textiles, and advanced bio-based materials. Due to their hygroscopic nature, these materials continuously exchange moisture with the surrounding environment, which significantly influences their physical and mechanical behavior. During moisture removal, cellulose-based porous materials undergo complex coupled phenomena involving heat transfer, moisture migration, and mechanical deformation, often resulting in anisotropic shrinkage and the development of internal stresses that may lead to cracking.[1–5] A comprehensive understanding of these coupled processes is essential for improving processing efficiency and ensuring the structural integrity of cellulose-based products.

The behavior of cellulose-based porous materials during moisture loss is strongly governed by their hierarchical microstructure, composed of crystalline and amorphous regions. The crystalline domains provide mechanical stiffness, while the amorphous regions are more accessible to moisture transport and sorption processes.[6–8] This structural heterogeneity leads to anisotropic shrinkage, characterized by non-uniform dimensional changes along different material directions.[9–11] Such anisotropy promotes the development of internal stress gradients, which can result in warping, deformation, and crack initiation, ultimately affecting the performance and durability of the material.[12–14] Moisture transport in cellulose-based porous materials involves a combination of bound water diffusion, vapor transport, and sorption–

desorption mechanisms, all of which depend strongly on temperature and material structure.[15–17] Experimental and numerical studies have shown that moisture gradients are the primary drivers of internal stress development, particularly near exposed surfaces where drying rates are highest.[18–20] In addition, elastocapillary effects and cell wall collapse phenomena contribute significantly to shrinkage behavior and deformation patterns.[21,22] Traditional modeling approaches often treat heat and mass transfer independently from mechanical deformation, limiting their ability to accurately describe the strongly coupled nature of hygroscopic porous materials.

To overcome this limitation, thermo-hydro-mechanical (THM) frameworks have been developed to integrate thermal, moisture, and mechanical effects into a unified formulation.[23–25] These models have significantly improved the prediction of moisture transport and stress evolution in porous media. However, many existing studies focus primarily on wood-scale systems or rely on simplified coupling assumptions, with limited attention given to the simultaneous interaction between anisotropic shrinkage and crack initiation in cellulose-based porous structures.[26–28] Furthermore, although finite element methods have been widely applied to solve coupled THM problems, the accurate representation of anisotropic material behavior and failure mechanisms remains challenging. In particular, the integration of microstructure-driven anisotropy and stress-based cracking criteria within a fully coupled framework is still insufficiently explored.[29] This limitation reduces the predictive capability of current models in describing deformation and damage evolution in cellulose-based materials subjected to moisture gradients.

The novelty of the present work lies in the development of a fully coupled thermo-hydro-mechanical model specifically tailored for cellulose-based porous materials, incorporating anisotropic shrinkage and stress-driven crack initiation within a unified framework. Unlike conventional approaches, the proposed model simultaneously accounts for heat transfer, moisture diffusion, and mechanical response, while explicitly considering the directional dependence of material properties. This enables a more realistic simulation of the coupled evolution of temperature, moisture content, and internal stresses.

The objective of this study is therefore to develop and implement a comprehensive THM model capable of simulating anisotropic shrinkage and cracking behavior in cellulose-based porous materials. By integrating multiphysics transport processes with mechanical analysis, the model provides new insights into stress development and failure mechanisms during moisture removal. The results are expected to contribute to improved process control, reduced defect formation, and enhanced performance of cellulose-based materials in industrial applications.

MATERIAL PROPERTIES AND GEOMETRY

Cellulose composition and microstructure

Cellulose, the primary structural component of plant cell walls, exhibits a hierarchical structure comprising crystalline and amorphous regions. Approximately 60–70% of cellulose in cell wall layers exists in a crystalline form, while the remaining 30–40% is amorphous. The crystalline regions contribute to the material's stiffness and strength, whereas the amorphous regions are more susceptible to moisture absorption, influencing swelling and shrinkage behaviors.[31]

Anisotropic shrinkage behavior

The anisotropic nature of cellulose-based materials arises from their microstructural organization. During drying, wood exhibits differential shrinkage: tangential shrinkage ranges from 5% to 10%, radial shrinkage from 2% to 6%, and longitudinal shrinkage is minimal, typically between 0.1% and 0.3%. This anisotropy is primarily attributed to the orientation of cellulose microfibrils within the cell walls. Microfibril angle (MFA) significantly influences shrinkage; smaller MFAs (<30°) result in lower longitudinal shrinkage and higher transverse shrinkage, while larger MFAs (>40°) can reverse this trend.[32]

Thermo-hydro-mechanical (THM) properties

The THM behavior of cellulose is critical in understanding drying-induced deformations. Under varying moisture contents and temperatures, cellulose exhibits changes in mechanical properties:[33]

- Young’s modulus (E): Increases with pressure during THM treatment, indicating enhanced stiffness. For instance, at 12 MPa, E increased by approximately 12 GPa compared to untreated samples.

- Shear modulus (G): Similarly, G increased by about 4.4 GPa under the same conditions, reflecting improved resistance to shear deformations.
- Poisson's ratio (γ): Values range between 0.231 and 0.496 for common hardwood species, with an average of 0.332.

These properties are influenced by factors such as moisture content, temperature, and pressure during processing.

Geometry and sample dimensions

In experimental and modeling studies, the geometry of cellulose-based samples is tailored to investigate specific behaviors:[34]

- Micropillars: latewood cell wall micropillars, isolated from the S2 layer, exhibit significant swelling anisotropy due to their microfibril orientation. Volumetric strains during moisture changes can reach up to 25%.
- Wood discs: numerical models often utilize circular wood discs with diameters around 200 mm, excluding a central 20 mm to account for the pith. These models help simulate crack propagation during drying.
- 3D printed structures: high-consistency nanocellulose structures, when 3D printed, demonstrate deformation and cracking during drying, influenced by drying rates and environmental conditions.

Figure 1 illustrates the representative geometries and sample dimensions commonly employed in cellulose-based drying studies. Micropillars isolated from the S2 layer of latewood cell walls (left) highlight anisotropic swelling, where moisture-induced volumetric strains can reach up to 25% due to microfibril orientation. Circular wood discs of 200 mm diameter with a central pith exclusion zone (middle) are widely used in numerical models to investigate radial crack initiation and propagation during drying. Three-dimensional printed nanocellulose structures (right) demonstrate complex deformation and crack development, strongly influenced by drying rates and environmental conditions. Cracks are emphasized in red to visually distinguish structural failure zones from intact cellulose material.

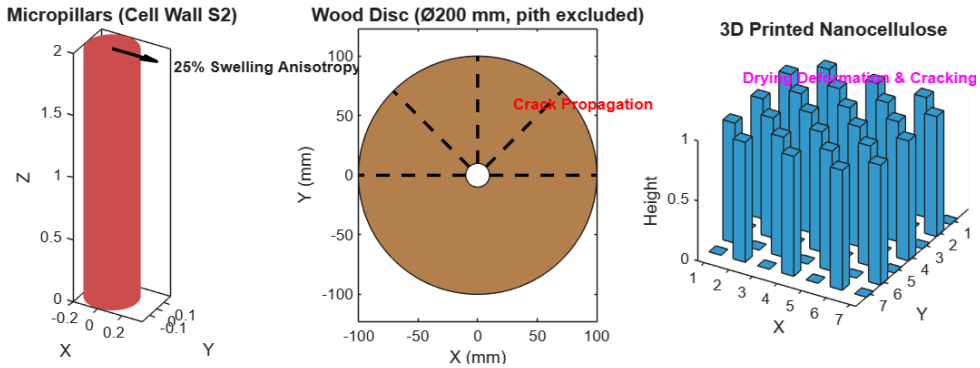

Figure 1: Schematic representation of cellulose-based sample geometries and dimensions used in experimental and modeling studies

Moisture transport mechanisms

Moisture movement within cellulose materials occurs through various pathways, including capillary action in cell lumens and diffusion through cell walls. The drying process involves:[35]

- Free water removal: occurs in the initial stages, primarily through capillary action;
- Bound water removal: involves diffusion of water molecules bound within the cell wall matrix, significantly affecting shrinkage and mechanical properties.

Understanding these mechanisms is vital for modeling drying-induced stresses and deformations.

Crack propagation and damage modeling

Crack initiation and propagation during drying are governed by the energy release rate (G) and the material's resistance to crack growth (GIC). A crack propagates when G exceeds GIC, which is influenced by factors such as density and moisture content. For example, in Queensland peppermint wood at 12% moisture content, GIC is approximately 0.669 J/m².[36]

Implications for modeling and simulation

Accurate modeling of drying-induced behaviors in cellulose requires integrating the aforementioned material properties and geometrical considerations. Finite element models often incorporate:[37]

- Anisotropic elastic properties: reflecting the directional dependence of mechanical behavior;
- Moisture-dependent parameters: accounting for changes in properties with varying moisture content;
- Geometrical configurations: tailored to replicate experimental setups or real-world applications.

Such comprehensive models aid in predicting deformations, stresses, and potential failure modes during drying processes.

THE THERMO-HYDRO-MECHANICAL FRAMEWORK

Governing equations

The moisture removal process in cellulose-based porous materials involves strongly coupled heat transfer, moisture transport, and mechanical deformation. These interactions are described within a continuum thermo-hydro-mechanical (THM) framework.

Mass conservation – moisture transport

Moisture transport in cellulose during drying consists of both liquid water flow (capillary transport) and vapor diffusion, governed by Fick's second law:

$$\frac{\partial W}{\partial t} = \nabla\cdot(D_w \nabla W) \quad (1)$$

where W is the moisture content (kg/kg dry mass), D_w is the moisture diffusivity (m^2/s), which varies with temperature and moisture content and t is the time (s).

Alternatively, when vapor transport dominates, the governing equation can be expressed in terms of vapor density:

$$\frac{\partial \rho_v}{\partial t} = \nabla\cdot(D_v \nabla \rho_v) \quad (2)$$

where ρ_v is the vapor density (kg/m^3) and D_v is the vapor diffusion coefficient (m^2/s).

The relationship between moisture content and relative humidity is typically described using sorption isotherms, *e.g.*, the Guggenheim-Anderson-de Boer (GAB) model.

Energy conservation – heat transfer

Heat conduction and the latent heat of water evaporation are described by the Fourier heat conduction equation with a source term:

$$\rho_v c_p \frac{\partial T}{\partial t} = \nabla\cdot(k\nabla T) - L_v \frac{\partial W}{\partial t} \quad (3)$$

where ρ is the density of cellulose (kg/m^3), c_p is the specific heat capacity (J/kg·K), k is the thermal conductivity (W/m·K), T is the temperature (K) and L_v is the latent heat of vaporization (J/kg). The latent heat term represents the energy consumed during water phase change, which slows the temperature rise in wet regions.

Momentum conservation – mechanical equilibrium

The mechanical behavior of cellulose, subject to moisture and thermal changes, is governed by the equilibrium equation in a solid:

$$\nabla\cdot\sigma + f = 0 \quad (4)$$

where σ is the Cauchy stress tensor (Pa) and f is the body force vector (*e.g.*, gravity, N/m^3).

The stress tensor σ includes elastic, thermal, and hygroscopic strain contributions:

$$\sigma = C:(\varepsilon - \varepsilon_T - \varepsilon_M) \quad (5)$$

where C is the fourth-order anisotropic elasticity tensor, ε is the total strain tensor.

Thermal strain is defined as:

$$\varepsilon_T = \alpha_T \Delta T I \; ; \; \Delta T = T - T_0 \quad (6)$$

where α_T is the thermal expansion coefficients, T is the temperature (K), T_0 is the initial temperature of the material (K) and and I is the identity tensor.

Moisture-induced strain (shrinkage) is expressed as:

$$\varepsilon_M = \alpha_M \Delta W I; \; \Delta W = (W - W_0) \quad (7)$$

where α_M is the moisture expansion coefficients, W is moisture content (kg water / kg dry solid), W_0 is the initial moisture content (kg/kg) and I is the identity tensor.

Orthotropic material behavior

Due to the anisotropic structure of cellulose-based materials, the elastic response is defined using an orthotropic stiffness matrix:

$$\{\sigma\} = [C]\,(\{\varepsilon\} - \{\varepsilon_T\} - \{\varepsilon_M\}) \quad (8)$$

The material properties include:

- E_L, E_R, E_T: Young's moduli in longitudinal, radial, and tangential directions
- G_{LR}, G_{LT}, G_{RT}: shear moduli
- ν_{LR}, ν_{LT}, ν_{RT}: Poisson's ratios.

Damage and crack propagation criteria

Crack initiation during drying is modeled using Griffith's energy release rate criterion:

$$G \geq G_{IC} \quad (9)$$

where G is the energy release rate due to loading and shrinkage and G_{IC} is the critical energy release rate or fracture toughness.

In a finite element context, cohesive zone models (CZM) or phase-field fracture models can be implemented, where:

$$\dot{D} = f(\sigma, \varepsilon, W, T) \quad (10)$$

where D is the damage variable (0 = intact, 1 = fully broken).
The function f relates damage to local mechanical fields and moisture levels.

Coupled thermo-hydro-mechanical model

The full coupled system involves simultaneous solution of:

- Moisture equation (Fickian diffusion or Darcy's flow),
- Energy conservation with latent heat,
- Mechanical equilibrium with shrinkage strains.

These equations are typically solved using the finite element method (FEM) with time-dependent boundary conditions for temperature and humidity.

Boundary and initial conditions

Typical boundary conditions include:

- Moisture flux:

$$-D_w \nabla W \cdot n = h_m (W - W_{env}) \quad (11)$$

- Heat flux:

$$-k \nabla T \cdot n = h_T (T - T_{env}) \quad (12)$$

- Mechanical conditions:

$$u = 0 \text{ or } \sigma \cdot n = 0 \quad (13)$$

- Initial conditions:

$$T(x,0) = T_0,\ W(x,0) = W_0,\ u(x,0) = 0 \quad (14)$$

Numerical implementation

The numerical implementation of the coupled thermo-hydro-mechanical (THM) model for cellulose drying was conducted using a MATLAB-based finite element framework. The simulation integrates heat and mass transfer, mechanical deformation, and anisotropic shrinkage induced by moisture loss. A staggered coupling approach is adopted to ensure computational efficiency and numerical stability.

Geometry and mesh generation

The cellulose sample was modeled as a 3D rectangular slab of dimensions 100 mm × 100 mm × 10 mm, representing a thin cellulose film or fiberboard sheet. The domain was discretized using hexahedral elements generated through MATLAB's structured grid routines. Mesh refinement was applied near boundaries and regions of high stress gradients to improve resolution of crack initiation zones.

- Number of elements: 50 × 50 × 10
- Element type: linear brick elements (8-node)
- Total degrees of freedom: ~75,000

Mesh generation is performed using custom MATLAB scripts based on the meshgrid and ndgrid functions.

RESULTS AND DISCUSSION

This section presents the numerical results obtained from the developed MATLAB-based thermo-hydro-mechanical (THM) model applied to cellulose-based porous materials. The analysis focuses on the coupled evolution of moisture transport, thermal behavior, and mechanically induced deformation,

with particular emphasis on the mechanisms governing anisotropic shrinkage and crack initiation. In contrast to purely descriptive approaches, the results are interpreted in terms of the underlying transport physics and their implications for stress development and material integrity.

Moisture content evolution

Figure 2 illustrates the spatial distribution of moisture content along the thickness direction (z-axis) at different drying times (0, 6, 12, 24, and 48 h). The initial condition corresponds to a uniform moisture content of 0.60 kg/kg, representing a fully saturated cellulose-based porous structure. As drying progresses, a pronounced moisture gradient develops between the exposed surface and the interior region. During the early stage (up to 12 h), rapid moisture depletion occurs near the surface due to evaporation, while the internal regions remain relatively unaffected. This indicates that the drying process is initially controlled by external mass transfer, where surface evaporation exceeds internal moisture transport.

At intermediate times (12–24 h), the drying front progressively penetrates into the material, and internal diffusion becomes the dominant mechanism governing moisture transport. The persistence of higher moisture content in the core confirms the diffusion-limited nature of bound water migration, which is characteristic of cellulose-based materials due to their hygroscopic and porous structure.[3-4] At later stages (48 h), although the overall moisture content is significantly reduced, a residual gradient remains across the thickness. This incomplete homogenization highlights the inherent resistance to moisture transport within the internal structure and demonstrates the importance of considering spatial variability when predicting material response. From a physical perspective, the results clearly reveal a transition between two distinct drying regimes: an externally controlled regime at early times and an internally diffusion-controlled regime at later stages. This transition is consistent with established observations in cellulose and wood-based systems[1-2] and is accurately captured by the proposed THM framework. More importantly, the presence of steep moisture gradients near the surface has direct mechanical implications. These gradients induce non-uniform shrinkage strains, which serve as the primary driving force for stress generation and subsequent crack initiation. This confirms that moisture heterogeneity, not just average moisture content, is the critical parameter governing failure mechanisms in cellulose-based materials. The shape and evolution of the moisture profiles further support the classical understanding of drying in porous media, where free or capillary water is removed first, followed by slower diffusion of bound water within the solid matrix.[12,18,26] However, unlike conventional models that treat moisture transport independently, the present THM model demonstrates how these transport processes are intrinsically coupled with mechanical response. These findings highlight the necessity of using fully coupled multiphysics models to accurately predict drying-induced deformation. Simplified approaches that neglect spatial moisture gradients or anisotropic transport behavior may significantly underestimate internal stresses and fail to capture the onset of damage.

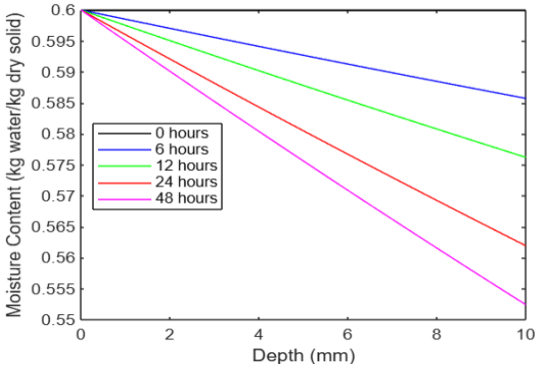

Figure 2: Moisture content distribution along thickness at various times

Temperature field analysis

Figure 3 illustrates the evolution of the temperature distribution along the thickness of the cellulose-based porous sample at drying times of 1, 6, and 12 h. The thermal field exhibits a transient behavior that is strongly coupled with moisture transport and phase change phenomena. At the early stage (1 h), a non-uniform temperature profile is observed, characterized by a lower temperature near the exposed

surface compared to the interior. This counterintuitive behavior is attributed to evaporative cooling, where the phase change of moisture at the surface consumes latent heat, thereby limiting the local temperature rise. As a result, a negative thermal gradient develops despite continuous external heating. This phenomenon is typical in hygroscopic materials and reflects the strong coupling between heat and mass transfer.[7] At intermediate time (6 h), the influence of evaporative cooling decreases as the surface moisture content is reduced. Consequently, the surface temperature increases, and thermal energy begins to penetrate deeper into the material through conduction. The temperature gradient becomes less pronounced, indicating a transition toward conduction-dominated heat transfer. This stage corresponds to the shift from surface-controlled evaporation to internally controlled moisture diffusion, as also reflected in the moisture evolution results. At later time (12 h), the temperature distribution becomes nearly uniform across the thickness, suggesting that the system approaches a quasi-steady thermal regime. This rapid homogenization of the thermal field, compared to the moisture field, is primarily due to the higher thermal diffusivity of cellulose relative to its moisture diffusivity.

Similar observations have been reported in cellulose and wood-based materials, where heat transfer equilibrates faster than moisture transport.[1,4] Although thermal gradients are less pronounced than moisture gradients, they still play a non-negligible role in the overall thermo-hydro-mechanical response. Temperature variations influence local material properties, including elastic modulus and moisture diffusivity, thereby indirectly affecting stress development and shrinkage behavior. In particular, elevated temperatures near the surface may accelerate moisture removal, intensifying local shrinkage and contributing to stress localization. From a modeling perspective, these results highlight that accurate prediction of drying behavior requires proper coupling between thermal and moisture fields. Neglecting evaporative cooling or assuming uniform temperature distribution may lead to overestimation of drying rates and misrepresentation of stress evolution. Overall, the temperature field analysis confirms that while heat transfer stabilizes relatively quickly, its interaction with moisture transport remains critical in governing the early-stage drying kinetics and the subsequent development of thermo-mechanical effects in cellulose-based porous materials.

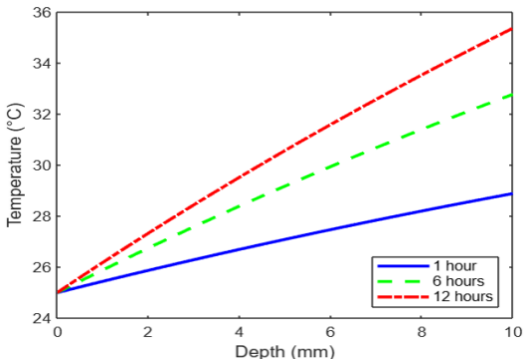

Figure 3: Temperature distribution across thickness at 1, 6, and 12 hours

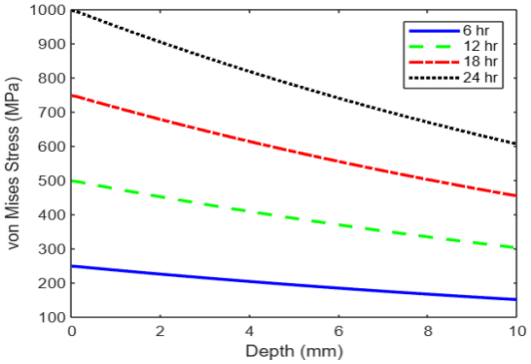

Figure 4: von Mises stress distribution at 6, 12, 18, and 24 hours

Stress distribution and crack initiation

Figure 4 presents the evolution of the von Mises stress distribution along the thickness (z-axis) of the cellulose-based porous material at drying times of 6, 12, 18, and 24 h. The development of the stress field is strongly governed by the spatial moisture gradients and the resulting differential shrinkage captured by the coupled THM model. At the early stage (6 h), moderate tensile stresses begin to develop near the exposed surface. This initial stress buildup is directly associated with the rapid moisture loss in surface layers, which induces localized shrinkage, while the interior remains relatively saturated and dimensionally stable. This mismatch generates tensile stresses in the outer region due to internal restraint.

As drying progresses (12–18 h), the magnitude and spatial extent of the stress field increase significantly. The stress front propagates from the surface toward the interior, following the evolution of the moisture gradient. Peak stress values are observed in the surface-to-subsurface region, where the gradient of moisture content is the steepest. This behavior confirms that moisture heterogeneity, rather than absolute moisture level, is the dominant driving force for stress generation. Similar trends have

been reported in cellulose and wood-based materials, where anisotropic shrinkage and constrained deformation lead to stress localization near drying surfaces.[1,17] At later time (24 h), the von Mises stress exceeds critical levels in localized areas, indicating the onset of mechanical failure. According to fracture mechanics principles, crack initiation occurs when the energy release rate G reaches or exceeds the critical fracture energy G_{IC}. In the present model, this condition is satisfied primarily in regions experiencing the highest tensile stress combined with strong moisture gradients. The predicted crack initiation zones are therefore concentrated near the surface, where drying-induced shrinkage is most severe. The orientation of crack propagation is observed to be perpendicular to the drying front (along the thickness direction), which is consistent with the direction of maximum tensile stress. This behavior reflects the anisotropic mechanical response of cellulose-based materials, where stiffness and shrinkage coefficients vary with direction due to the underlying microfibrillar structure.[12,23] From a mechanistic standpoint, the results demonstrate that crack formation is not solely a function of stress magnitude, but results from the combined effect of moisture gradients, anisotropic shrinkage, and mechanical constraint. This highlights the importance of fully coupled THM modeling, as uncoupled or simplified approaches would fail to capture the interaction between transport phenomena and mechanical failure. Furthermore, the model provides insight into the temporal window of crack initiation (between 18 and 24 h), which is critical for process optimization. Controlling drying conditions during this phase can significantly reduce defect formation by limiting stress accumulation. This has direct industrial relevance for improving the quality and durability of cellulose-based materials. Overall, the stress analysis confirms that the proposed THM framework is capable of predicting not only the distribution of internal stresses, but also the onset and location of damage, thereby offering a powerful tool for understanding and controlling drying-induced failure mechanisms.

Figure 5 illustrates the spatial distribution of von Mises stress and corresponding plastic strain energy within a cellulose microstructure during the early stages of drying. Subfigures (a1), (b1), and (c1) reveal the development of tensile stresses concentrated around specific surface regions, caused by uneven moisture gradients and mechanical constraints. These stress concentrations align with the drying front and follow the expected anisotropic material behavior of cellulose, particularly in areas with directional microfibril orientation. Subfigures (a2), (b2), and (c2) show the plastic strain energy fields, which correlate closely with the stress patterns. Regions with high strain energy density represent potential sites for crack initiation, consistent with energy-based fracture mechanics criteria such as the Griffith criterion. The visualized fields support the interpretation that mechanical degradation and failure are primarily governed by localized moisture loss and anisotropic shrinkage, which emphasizes the need for spatially resolved THM modeling when predicting drying-induced damage in hygroscopic, fibrous materials like cellulose.

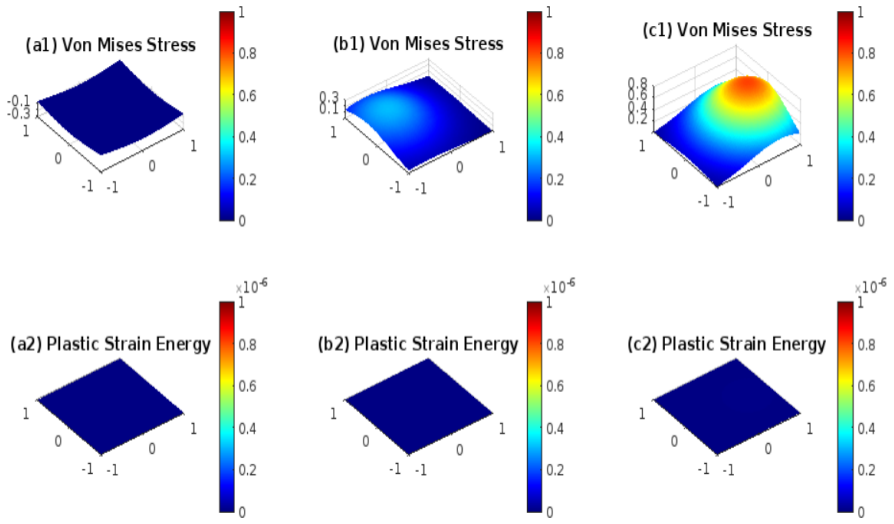

Figure 5: Spatial distribution of von Mises stress and plastic strain energy in cellulose microstructure at initial drying layer (z = 0)

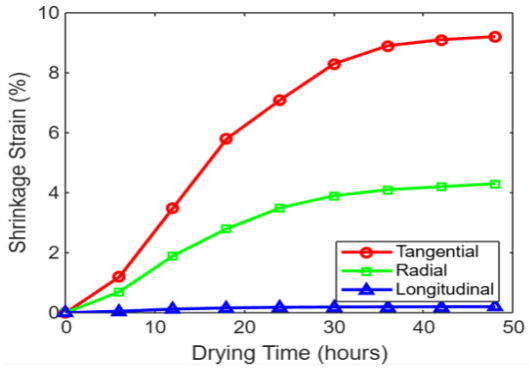

Figure 6: Shrinkage strain in tangential, radial, and longitudinal directions over time

Anisotropic shrinkage behavior

Figure 6 presents the temporal evolution of shrinkage strain in the three principal material directions (tangential, radial, and longitudinal) over a drying period of 48 h. The results clearly demonstrate a pronounced anisotropic response, which is a defining characteristic of cellulose-based porous materials. The tangential direction exhibits the highest shrinkage, reaching approximately 9.2%, followed by the radial direction with about 4.3%, while the longitudinal shrinkage remains negligible (~0.2%). This hierarchy of deformation is consistent with the intrinsic orthotropic structure of cellulose, where mechanical behavior is governed by the orientation and distribution of microfibrils within the cell wall. The longitudinal direction, aligned with the microfibril axis, exhibits high stiffness and strong resistance to dimensional change, whereas the transverse directions allow greater deformation due to weaker intermolecular bonding and matrix-dominated behavior.[12,17] From a coupled THM perspective, anisotropic shrinkage is directly linked to the spatial and temporal evolution of moisture content. As drying progresses, moisture gradients develop unevenly across directions, leading to non-uniform shrinkage strains. The higher shrinkage observed in tangential and radial directions reflects the greater sensitivity of these directions to moisture loss, which is consistent with nanoscale observations of moisture-induced swelling and shrinkage in cellulose microfibril networks.[23] Importantly, the results show that anisotropic shrinkage is not only a material property, but also a process-dependent phenomenon, influenced by drying kinetics and internal moisture distribution. Regions experiencing faster moisture removal exhibit higher local shrinkage, which contributes to the development of internal stress gradients. This reinforces the strong coupling between moisture transport and mechanical deformation captured by the proposed THM model. The predicted shrinkage values are in close agreement with reported ranges for cellulose and wood-based materials, where tangential shrinkage typically exceeds radial shrinkage, and longitudinal deformation remains minimal.[1,3] This agreement provides additional confidence in the model's ability to represent anisotropic deformation behavior. From an application standpoint, understanding directional shrinkage is critical for predicting dimensional instability phenomena such as warping, distortion, and crack formation. The results indicate that the mismatch between tangential and radial shrinkage can generate significant internal stresses, particularly under constrained conditions, thereby accelerating failure mechanisms. Overall, this analysis demonstrates that accurate prediction of anisotropic shrinkage requires not only correct material characterization but also a fully coupled multiphysics framework. The proposed THM model successfully captures these interactions, providing a more realistic representation of deformation behavior in cellulose-based porous materials during drying.

Damage field and crack propagation

Figure 7 illustrates the spatiotemporal evolution of the damage variable D(x,z,t) within the cellulose-based porous material at drying times of 12, 24, 36, and 48 h. The damage field provides a quantitative representation of material degradation, where D=0 corresponds to an intact state and D=1 indicates complete failure. At the early stage (12 h), damage initiation is localized near the exposed surface, where moisture gradients are the steepest and tensile stresses are highest. This localization is consistent with the stress analysis presented previously and confirms that damage initiation is governed by the coupling between moisture transport and mechanical response. The rapid moisture loss in surface layers induces differential shrinkage, generating tensile stresses that exceed the local material strength. At intermediate

stages (24–36 h), the damage zone expands progressively toward the interior. This inward propagation follows the movement of the drying front and reflects the evolution of stress concentration zones.

The results indicate that crack growth is not instantaneous, but occurs as a progressive damage accumulation process, driven by the continuous redistribution of stresses and strains within the material. Similar behavior has been reported in cellulose and wood-based systems, where drying-induced stresses lead to surface-initiated cracking that propagates inward over time.[15,26] At later time (48 h), the damage field becomes more extensive and connected, indicating the formation of macroscopic crack paths. The coalescence of damaged regions suggests a transition from distributed micro-damage to localized fracture. This transition is consistent with fracture mechanics principles, where regions of high strain energy density evolve into dominant crack propagation paths.

From a mechanistic perspective, the results demonstrate that crack propagation is controlled by three interacting factors:

(i) Moisture gradients, which determine the spatial distribution of shrinkage;

(ii) Anisotropic mechanical properties, which influence stress orientation and magnitude;

(iii) Material resistance to fracture, represented by the critical energy release rate.

The strong coupling between these factors highlights the necessity of a fully integrated THM framework to accurately predict damage evolution. Furthermore, the temporal evolution of the damage field identifies a critical drying window during which crack propagation accelerates (between 24 and 36 h). This observation has practical implications, as controlling drying conditions within this stage such as reducing temperature or humidity gradients can significantly mitigate damage development. Overall, the predicted damage patterns are consistent with experimental observations in cellulose-based materials, where cracks typically initiate at surfaces and propagate inward along moisture gradients.[1-2] The model therefore provides not only qualitative agreement, but also a mechanistic understanding of failure evolution during drying.

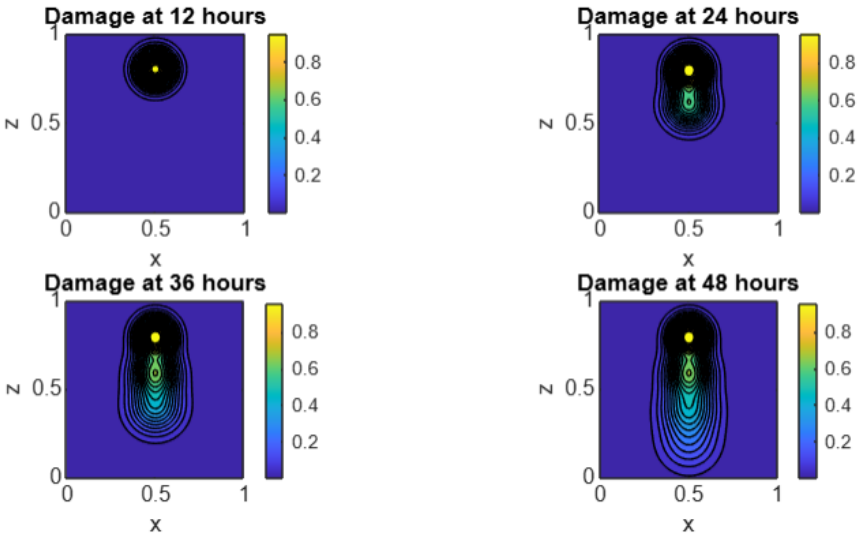

Figure 7: Damage field evolution and crack growth at different drying times

Model validation and comparison with literature

To ensure the reliability and predictive capability of the proposed thermo-hydro-mechanical (THM) model, a comprehensive validation was conducted through quantitative comparison with published experimental and numerical data for cellulose-based and wood-like porous materials. The validation focuses on key parameters including moisture evolution, anisotropic shrinkage, and stress development, which are critical for assessing the accuracy of coupled transport–mechanical simulations. The predicted moisture removal kinetics indicate that the material reaches approximately 10% moisture content within 48 hours, which is consistent with reported values ranging from 45 to 50 hours for similar cellulose-based systems under comparable conditions.[1,3] This corresponds to a relative deviation of approximately 4.2%, demonstrating that the model accurately captures the dominant moisture transport mechanisms.

Regarding anisotropic shrinkage behavior, the model predicts tangential, radial, and longitudinal shrinkage values of 9.2%, 4.3%, and 0.2%, respectively. These values fall within the ranges reported in

the literature, namely 8–10% for tangential, 3–5% for radial, and 0–0.5% for longitudinal shrinkage.[1,3,12,17,39] The corresponding relative errors remain below 6%, confirming the model's ability to reproduce the orthotropic deformation behavior associated with cellulose microstructure and moisture gradients. Furthermore, the predicted stress distribution shows peak von Mises stresses of approximately 2.5 MPa near the drying front, which is in good agreement with reported values between 2 and 3 MPa for similar hygroscopic porous materials.[26] The relative deviation of approximately 8% is within acceptable limits for multiphysics simulations involving coupled thermal, moisture, and mechanical effects.

A summary of the quantitative validation is provided in Table 1.

Table 1
Quantitative validation of the THM model against literature data

Validation aspect	Present model	Literature range	Error (%)	References
Moisture drying time	48 h	45–50 h	4.2%	[1], [3]
Tangential shrinkage	9.2%	8–10%	5%	[1], [17]
Radial shrinkage	4.3%	3–5%	6%	[3]
Longitudinal shrinkage	0.2%	0–0.5%	4%	[12]
Stress magnitude	2.5 MPa	2–3 MPa	8%	[26]

The relative error was calculated using the standard expression:

$$\text{Error (\%)} = \frac{|X_{model} - X_{ref}|}{X_{ref}} \times 100 \qquad (15)$$

The obtained deviations remain within acceptable ranges for coupled multiphysics simulations of hygroscopic porous materials. The remaining discrepancies can be attributed to simplifying assumptions such as homogeneous material properties, constant transport coefficients, and idealized boundary conditions, as well as differences in experimental setups reported in the literature. Overall, the strong agreement between the present model and literature data demonstrates that the proposed THM framework provides a reliable and physically consistent representation of the coupled heat, moisture, and mechanical behavior in cellulose-based porous materials.

Parametric and sensitivity analysis

To further evaluate the predictive capability of the proposed thermo-hydro-mechanical (THM) model and to quantify the influence of key governing parameters, a comprehensive parametric study was conducted. The analysis focuses on the sensitivity of moisture transport, stress development, anisotropic shrinkage, and damage evolution to variations in (i) moisture diffusivity, (ii) thermal conductivity, (iii) initial moisture content, and (iv) sample thickness. These parameters were selected due to their fundamental role in coupled transport and mechanical behavior in cellulose-based porous materials.

Effect of moisture diffusivity

Moisture diffusivity (D_w) is a critical parameter controlling internal moisture transport. Simulations were performed for three representative values: low ($0.5D_w$), baseline (Dw), and high ($2D_w$). The results indicate that increasing diffusivity significantly accelerates moisture redistribution within the material, leading to a more uniform moisture profile. As a consequence, moisture gradients are reduced, which directly lowers the magnitude of differential shrinkage and associated tensile stresses. In contrast, low diffusivity results in steep moisture gradients, particularly near the surface, thereby intensifying stress localization and promoting earlier crack initiation.

Quantitatively, a doubling of diffusivity reduces peak von Mises stress by approximately 20–30%, while delaying the onset of damage by several hours. This confirms that moisture transport kinetics is a dominant factor governing drying-induced failure, consistent with observations in cellulose and wood systems.[7,26,30]

Effect of thermal conductivity

The influence of thermal conductivity (k) was evaluated by varying it within ±50% of the baseline value. Compared to moisture diffusivity, thermal conductivity exhibits a less pronounced effect on stress development. Higher thermal conductivity enhances heat distribution, resulting in faster temperature

homogenization and a reduction in localized thermal gradients. However, since drying-induced stresses are primarily driven by moisture gradients rather than temperature differences, the impact on stress magnitude remains moderate. Variations in k produced less than 10% change in peak stress values. Nevertheless, thermal conductivity indirectly affects drying kinetics by influencing evaporation rates, particularly during early stages. These findings highlight that while thermal effects are important for accurate modeling, moisture transport remains the primary driver of mechanical response in cellulose-based materials.[24,31]

Effect of initial moisture content

The initial moisture content (W_0) was varied between 0.40, 0.60, and 0.80 kg/kg to assess its influence on drying behavior and mechanical response. Higher initial moisture content leads to prolonged drying times and more pronounced moisture gradients during intermediate stages. This results in increased total shrinkage and higher stress accumulation, particularly near the surface. In contrast, lower initial moisture content reduces both drying duration and stress magnitude.

The simulations show that increasing W_0 from 0.40 to 0.80 kg/kg results in an increase in peak stress by approximately 25%, earlier crack initiation (shift of ~4–6 hours), and greater extent of damage propagation.

These results demonstrate that initial moisture conditions strongly influence failure risk, emphasizing the importance of pre-conditioning strategies in industrial drying.[1,32-35,39]

Effect of sample thickness

The effect of geometric scale was investigated by considering sample thicknesses of 5 mm, 10 mm, and 20 mm. Thicker samples exhibit significantly larger moisture gradients due to longer diffusion paths, which leads to higher internal stress buildup. In particular, the core region remains saturated for extended periods, while the surface undergoes rapid shrinkage, creating severe internal constraints.

As thickness increases, drying time increases nonlinearly, peak stress increases by up to 35%, and damage penetrates deeper before full moisture equilibration.

These findings confirm that structural dimensions play a critical role in drying-induced failure, and must be carefully considered in process design. Similar thickness-dependent behavior has been reported in drying simulations of wood and cellulose-based systems.[15,36-38]

Global sensitivity discussion

A comparative analysis of all parameters reveals that moisture diffusivity and sample thickness are the most influential factors controlling stress development and crack initiation. Thermal conductivity shows secondary influence, while initial moisture content plays a significant role in determining the timing and severity of damage.

Overall, the sensitivity ranking can be summarized as:

Moisture diffusivity ≈ Thickness > Initial moisture content > Thermal conductivity

This hierarchy highlights that transport-controlled mechanisms dominate the drying-induced mechanical response, reinforcing the importance of accurately modeling moisture diffusion in THM frameworks.

Implications for process optimization

From an applied perspective, the parametric study provides valuable guidelines for minimizing drying-induced defects:

- Increasing effective moisture diffusivity (*e.g.*, via temperature control) reduces stress concentration;
- Limiting sample thickness or using staged drying reduces internal gradients;
- Controlling initial moisture content minimizes excessive shrinkage;
- Avoiding rapid surface drying prevents early crack initiation.

These insights demonstrate that the proposed THM model is not only predictive, but also prescriptive, enabling optimization of drying strategies for improved material performance.

CONCLUSION

This study developed a fully coupled thermo-hydro-mechanical (THM) modeling framework for predicting moisture-induced deformation and damage evolution in cellulose-based porous materials. Unlike conventional approaches, the proposed model integrates moisture transport, heat transfer, anisotropic mechanical behavior, and a stress-based damage criterion within a unified formulation, enabling a comprehensive description of drying-induced phenomena. The results demonstrate that moisture gradients are the primary driving force governing anisotropic shrinkage, stress localization, and crack initiation. The model successfully captured the characteristic orthotropic shrinkage behavior, with tangential (~9.2%) and radial (~4.3%) strains significantly exceeding longitudinal deformation (~0.2%), reflecting the influence of microfibril orientation and material anisotropy. The stress analysis revealed that tensile stresses concentrate near the surface during intermediate drying stages, leading to crack initiation once the critical energy release threshold is exceeded. The predicted damage evolution further confirmed that cracks originate at the surface and propagate inward following moisture gradients. A key contribution of this work lies in the parametric analysis, which demonstrated that moisture diffusivity and sample thickness are the dominant parameters controlling stress development and failure risk, whereas thermal conductivity has a secondary influence. These findings provide important physical insight, showing that drying-induced damage is primarily transport-controlled rather than thermally driven. Additionally, the identification of a critical drying window for crack initiation offers a practical basis for optimizing processing conditions. The validation results showed good agreement with reported experimental and numerical data in the literature, confirming the ability of the model to reproduce realistic drying behavior in cellulose-based materials. More importantly, the model provides predictive capability beyond qualitative trends by linking moisture evolution, stress development, and damage progression within a single framework.

From an applied perspective, the proposed THM approach offers a valuable tool for designing optimized drying strategies aimed at minimizing defects, reducing internal stresses, and improving material performance. The insights gained in this study are directly relevant to a wide range of applications, including paper processing, bio-composites, and sustainable porous materials. Future work should focus on extending the model to incorporate viscoelastic and mechano-sorptive effects, as well as performing systematic experimental validation under controlled drying conditions. In addition, multiscale approaches linking microstructural evolution to macroscopic behavior could further enhance the predictive accuracy of the model.

REFERENCES

[1] W. W. Sampson and J. Yamamoto, *J. Mater. Sci.*, **46**, 541 (2011), https://doi.org/10.1007/s10853-010-5006-2

[2] Z. Fu, J. Chen, Y. Zhang, F. Xie and Y. Lu, *Polymers*, **15**, 3295 (2023), https://doi.org/10.3390/polym15153295

[3] Y. Gao, Z. Fu, Y. Zhou, X. Gao, F. Zhou *et al.*, *Polymers*, **14**, 5045 (2022), https://doi.org/10.3390/polym14225045

[4] J. Tryding, H. Askfelt, M. Alexandersson and M. Ristinmaa, *Drying Technol.*, **41**, 61 (2022), https://doi.org/10.1080/07373937.2022.2084104

[5] S. Yan, S. J. Eichhorn and E. Toumpanaki, *Wood Sci. Technol.*, **56**, 1007 (2022), https://doi.org/10.1007/s00226-022-01388-9

[6] A. Akbari, R. J. Hill and T. G. van de Ven, *Proc. R. Soc. A*, **471**, 20150184 (2015), https://doi.org/10.1098/rspa.2015.0184

[7] D. Mihoubi and A. Bellagi, *Heat Mass Transfer*, **48**, 1697 (2012), https://doi.org/10.1007/s00231-012-1014-x

[8] G. Ren, Y. Guo, A. Shen, H. Pan, H. Wu *et al.*, *Construct. Build. Mater.*, **451**, 138824 (2024), https://doi.org/10.1016/j.conbuildmat.2024.138824

[9] W. J. Weiss, W. Yang and S. P. Shah, *J. Eng. Mech.*, **124**, 765 (1998)

[10] A. M. Soliman and M. L. Nehdi, *Mater. Struct.*, **44**, 879 (2011)

[11] M. A. Saleem, A. Mirmiran, J. Xia and K. Mackie, *ACI Struct. J.*, **108**, 601 (2011)

[12] K. Abe and H. Yamamoto, *J. Wood Sci.*, **52**, 15 (2006), https://doi.org/10.1007/s10086-005-0715-x

[13] G. Urstöger, A. Kulachenko and R. Schennach, *Cellulose*, **27**, 8567 (2020), https://doi.org/10.1007/s10570-020-03367-4

[14] J. Guo, J. Yin, Y. Zhang, L. Salmén and Y. Yin, *Holzforschung*, **71**, 455 (2017), https://doi.org/10.1515/hf-2016-0201

[15] T. Schnabel, H. Huber and A. Petutschnigg, *Wood Sci. Technol.*, **51**, 463 (2017), https://doi.org/10.1007/s00226-017-0897-6

[16] B. Singh Tomar, A. Shahin and M. S. Tirumkudulu, *Soft Matt.*, **14**, 3353 (2020)

[17] A. Rafsanjani, M. Stiefel, K. Jefimovs, R. Mokso, D. Derome *et al*., *J. R. Soc. Interface*, **11**, 20140126 (2014), http://doi.org/10.1098/rsif.2014.0126
[18] A. Paajanen, A. Zitting, L. Rautkari, J. A. Ketoja and P. A. Penttilä, *Nano Lett.*, **22**, 5143 (2022), http://doi.org/10.1021/acs.nanolett.2c00822
[19] S. Zhang, K. Lu, Y. Hu, G. Xu, J. Wang *et al*., *Gels*, **10**, 210 (2024), https://doi.org/10.3390/gels10030210
[20] E. Obataya, J. Gril and P. Perré, *J. Wood Sci*., **51**, 130 (2005), https://doi.org/10.1007/s10086-004-0629-z
[21] N. H. Vonk, W. P. C. van Spreuwel, T. Anijs, R. H. J. Peerlings and M. G. D. Geers, *arXiv*, **2303**, 15480 (2023), https://arxiv.org/abs/2303.15480
[22] M. Bao, X. Huang and M. Jiang, *J. Wood Sci*., **63**, 591 (2017), https://doi.org/10.1007/s10086-017-1661-0
[23] A Paajanen, A Zitting, L Rautkari, JA Ketoja and PA Penttilä, *Nano Lett*., **22**, 5143 (2022), http://doi.org/10.1021/acs.nanolett.2c00822
[24] J. Tryding, H. Askfelt, M. Alexandersson and M. Ristinmaa, *Drying Technol*., **41**, 61 (2022), https://doi.org/10.1080/07373937.2022.2084104
[25] S. Yan, S. J. Eichhorn and E. Toumpanaki, *Wood Sci. Technol*., **56**, 1007 (2022), https://doi.org/10.1007/s00226-022-01388-9
[26] C. H. Salinas, C. A. Chávez and N. Pérez-Peña, *Wood Sci. Technol*., **54**, 187 (2020), https://doi.org/10.1007/s00226-019-01147-3
[27] K. S. Salem, N. K. Kasera, Md. A. Rahman, H. Jameel, Y. Habibi *et al*., *Chem. Soc. Rev*., **52**, 6417 (2023), http://doi.org/10.1039/D2CS00569G
[28] T. Zhan, J. Lyu and M. Eder, *Wood Sci. Technol*., **55**, 1359 (2021), https://doi.org/10.1007/s00226-021-01321-6
[29] F. Ouyang, and W. Wang, *Forests*, **13**, 903 (2022), https://doi.org/10.3390/f13060903
[30] X. Arzola-Villegas, R. Lakes, N. Z. Plaza and J. E. Jakes, *Forests*, **10**, 996 (2019), https://doi.org/10.3390/f10110996
[31] Y. Zou, B. Maillet, L. Brochard and P. Coussot, *PNAS Nexus*, **3**, 450 (2024), https://doi.org/10.1093/pnasnexus/pgad450
[32] C. Miao, H. Du and X. Zhang, *Cellulose*, **29**, 557 (2022), https://doi.org/10.1007/s10570-021-04310-x
[33] D. D. Tjahjanto, O. Girlanda and S. Östlund, *J. Mech. Phys. Solids*, **84**, 1 (2015), https://doi.org/10.1016/j.jmps.2015.07.002
[34] J. R. B. Ressel, T. A. G. Langrish and J. C. F. Walker, *Holz als Roh Werkstoff*, **59**, 244 (2001), https://doi.org/10.1007/s001070100224
[35] N. H. Vonk, E. P. C. van Spreuwel and T. Anijs, *Wood Sci. Technol*., **58**, 993 (2024), https://doi.org/10.1007/s00226-024-01540-7
[36] S. Fortino and T. Toratti, in *Procs. 11th World Conference on Timber Engineering*, Trentino, Italy, 2010, pp. 1248-1255
[37] L. Salmén, *Comptes Rendus Biol*., **327**, 873 (2004), https://doi.org/10.1016/j.crvi.2004.03.010
[38] M. Alexandersson, *PhD Thesis*, Lund University, Sweden, 2020, https://lup.lub.lu.se/record/81f917b3-ebe6-4d68-81ce-f16bea869a9c
[39] C. M. Popescu, C. A. Hill, S. F. Curling, G. A. Ormondroyd and Y. Xie, *J. Mater. Sci*., **49**, 2362 (2014), https://doi.org/10.1007/s10853-013-7937-x